The temperature dependence of vibronic spectra in irradiated silicon

1972 J. Phys. C: Solid State Phys. 5 1265

(http://iopscience.iop.org/0022-3719/5/11/021)

J. Phys. C: Solid State Phys., Vol. 5, 1972. Printed in Great Britain

The temperature dependence of vibronic spectra in irradiated silicon

A P G HARE, G DAVIES and A T COLLINS
Wheatstone Physics Laboratory, King's College, Strand, London WC2

MS received 3 February 1972

Abstract. Crucible grown and high purity floating zone silicon specimens have been irradiated at room temperature with γ rays. High resolution cathodoluminescence spectra of the vibronic bands with zero phonon lines at 0·717, 0·724, 0·790, 0·795, 0·898 and 0·969 eV are given. The widths and energies of these lines, and the intensities of the 0·790, 0·795 and 0·969 eV lines relative to the total intensities of their associated bands, are given in the temperature range 25 to 75 K. These data are discussed in terms of the theory of linear and quadratic electron–phonon coupling in the adiabatic approximation, using Debye spectra of coupled phonons and, for the 0·790, 0·795 and 0·969 eV lines, densities of coupled phonons derived from the emission band shapes. The theory gives a selfconsistency between the spectral band shapes and the widths and energies of the zero phonon lines, but does not satisfactorily fit the temperature dependence of the intensities of the zero phonon lines. It is not known whether the failure of the theory is due to a Jahn–Teller effect (no absorption at the centres has been detected), or to the coupling by the electron–phonon interaction of electronic states whose energies are not greatly separated compared with the phonon energies involved.

1. Introduction

Luminescence spectra from γ, neutron and electron irradiated silicon have been reported by several workers. After irradiation, all specimens will apparently show a luminescence band with a zero phonon line at 0·969 eV (Yukhnevitch 1965, Yukhnevitch and Tkachev 1966). Crucible grown specimens also show luminescence from a band with zero phonon lines at 0·790 and 0·795 eV (Spry and Compton 1965, Yukhnevitch *et al* 1967). The dependence of this system on the crucible grown origin of the specimens suggests the optical centre involved is at least partly due to oxygen. This is confirmed by the annealing behaviour of the band, which closely follows that of the K or G-15 EPR spectrum (Johnson and Compton 1971, Almeleh and Goldstein 1966). The annealing behaviour of the 0·969 eV band is similar to that of the divacancy (Johnson and Compton 1971, Watkins and Corbett 1965).

In this paper we report high resolution cathodoluminescence spectra from crucible grown silicon, and from floating zone purified silicon, after room temperature γ irradiation. The emission band shapes and their temperature dependence are reported over the range 25 to 75 K. These results are discussed in terms of the theory of vibronic spectra in the adiabatic approximation.

2. Experimental

Before irradiation, the crucible grown silicon used in this work has a resistivity of 0·5 Ω m and contains about 2×10^{24} m^{-3} oxygen impurities, whereas the floating zone purified silicon has a resistivity of 8 Ω m and contains less than 10^{22} m^{-3} oxygen. Radiation damage centres were created by exposing the samples to a total dose of 10^8 rad of γ radiation in the spent fuel pond at AERE Harwell. The luminescence was excited by a 50 kV electron beam with a mean beam current of 50 μA. The luminescence was collected from the excited face of the specimen and analysed by a Spex 1702 monochromator fitted with a 600 groove mm^{-1} grating blazed at 1·6 μm, and a PbS detector cooled to solid CO_2 temperature. The electron beam was electronically chopped at about 70 Hz and the alternating signal at the PbS detector was recovered using phase sensitive detection. Chopping the electron beam has two important advantages over chopping the luminescence. Firstly the stray radiation from the heated tungsten filament of the electron gun, which has a maximum infrared emission in the wavelength region being studied, does not give rise to an alternating signal at the detector. Secondly, for a given mean photon flux entering the spectrometer the heating of the sample by the electron beam is halved.

The temperature of the sample was controlled over the range 24 to 100 K using an Air Products AC-3L-110 'Cryotip' refrigerator with hydrogen as working gas, and over the range 5 to 30 K using a liquid helium cryostat fitted with a drip-feed valve. The magnitude of the beam heating was determined by mounting a thermocouple directly on one sample and measuring the difference between the sample and mount temperatures as a function of beam current.

The response function of the spectrometer and detector was determined by recording the spectrum from a strip tungsten filament lamp. Long-wavelength-pass filters were used to eliminate unwanted orders of diffraction. The temperature of the filament was measured with an optical pyrometer and the black body spectrum calculated after applying the correction factor for tungsten (Roberts and Miller 1960). Allowance was also made for the transmission characteristics of the filters which were measured on a spectrophotometer. The experimental emission spectra were all corrected for the response of the measuring system and transformed from a linear wavelength to a linear energy scale.

3. Results and discussion

3.1. The emission spectra

Figure 1 shows a typical emission obtained at 26 K from a sample of crucible grown, irradiated silicon. After irradiation the intrinsic luminescence (Dean *et al* 1967) is only very weakly observed. It does not interfere with the present measurement. The 0·969 eV zero phonon line is at the head of a band stretching to 0·8 eV. The sharp structure between 0·969 eV and 0·905 eV will be shown to arise from one phonon vibronic transitions associated with the 0·969 eV line. The sharp line at 0·897 eV is another zero phonon line, and not a localized mode replica of the 0·969 eV line. This is seen on studying the temperature dependence of the two lines (§ 3.2), for a harmonic local mode will give an emission line of the same width as the zero phonon line. At low temperatures the width of the 0·897 eV line is seen to be greater than that of the 0·969 eV line. If a local mode

phonon is involved it must, therefore, be anharmonic, so that it may be inhomogeneously broadened through coupling to lattice strains and homogeneously broadened by lifetime broadening. The lifetime broadening will increase with temperature as alternative channels for the decay of the local mode are created by the excitation of lattice modes.

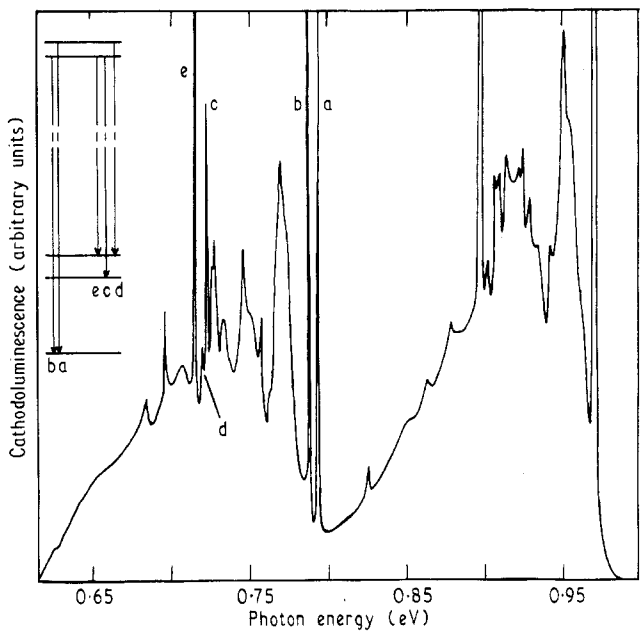

Figure 1. Cathodoluminescence spectrum from γ irradiated crucible grown silicon, taken at 26 K. Inset is an electronic energy level diagram for the lower energy emission (discussed in § 3.1).

In practice, the width of the 0·897 eV line increases slightly less than the 0·969 eV line (figure 2), showing that both are zero phonon lines. Spectral features at 0·88, 0·86, 0·85 eV are one phonon replicas of the 0·897 eV line (cf the structure below the 0·969 eV line). The emission between 0·969 and 0·80 eV is thus mainly composed of two vibronic bands with zero phonon lines at 0·897 and 0·969 eV. These lines have always been observed in the same ratio of 1:11, and so presumably occur at the same centre. Two further lines at 0·900 and 0·825 eV do not fit into this scheme.

The pair of zero phonon lines at 0·790, 0·795 eV thermalize in a way closely describable by the Boltzmann relation

$$\frac{I_1}{I_2} = r \exp\left(-\frac{E}{kT}\right)$$

where I_1, I_2 are the intensities of the 0·795, 0·790 eV lines. Good fits are obtained with $E = 4$ meV, $r = 1$ as observed by Jones and Compton (1971), or with the spectroscopically observed $E = 5{\cdot}2$ meV and $r \sim 0{\cdot}5$. At 24 K the 0·790 eV line is dominant. The structure between 0·80 and 0·72 eV is therefore predominantly due to one phonon vibronic transitions associated with this line. Further lines are seen at 0·717, 0·722 and 0·724 eV, apparently always with the 0·790, 0·795 eV doublet. The strongest, at 0·717 eV,

and the second strongest, at 0·724 eV, have a separation of 7·1 meV, which is different from the 0·790, 0·795 eV splitting (5·2 meV). The intensity ratio of the 0·717, 0·724 eV lines is $I_{717}/I_{724} = 2{\cdot}7 \pm 0{\cdot}1$ at 25 K, and is relatively temperature independent, indicating that the splitting occurs in the final states of the transitions. These facts are sufficient to show that the 0·717, 0·724 eV lines are not local mode replicas of the 0·790, 0·795 eV lines. A weak line is observed at 0·722 eV, 5·2 meV from the 0·717 eV line. These

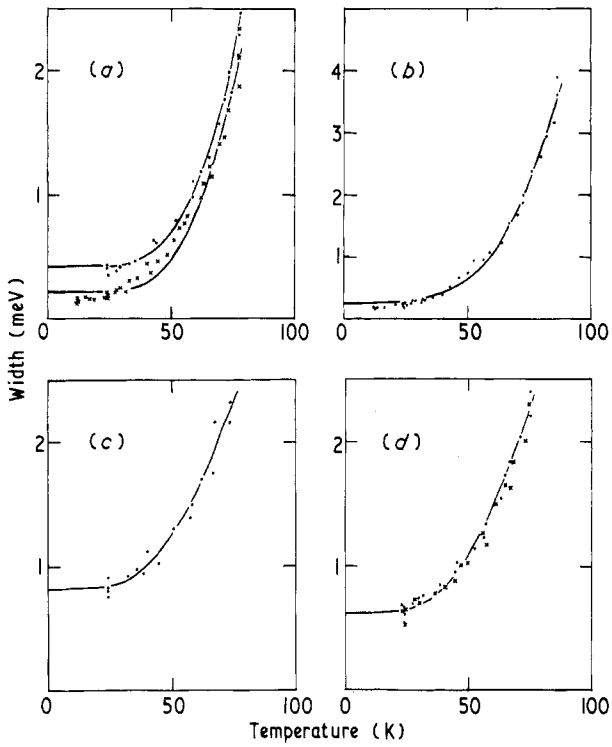

Figure 2. Measured and calculated full widths at half heights of zero phonon lines at (*a*) × 0·790, ● 0·795 eV, (*b*) 0·969 eV, (*c*) 0·898 eV, (*d*) ● 0·717, × 0·724 eV. In (*a*) and (*b*) the lines are calculated using the $\rho(w)$ shown in figure 6 and Debye spectra with cut off energies 22 and 15 meV respectively give closely similar lines. In (*c*) and (*d*) the calculation uses Debye spectra with cut off energies of 16 meV.

figures are consistent with an energy level scheme as in the inset of figure 1. The sharp 0·759 eV line is a zero phonon line of another centre: on annealing its strength increases while the emission shown in figure 1 disappears.

The emission between 0·80 and 0·61 eV is thus mainly associated with two pairs of zero phonon lines at 0·790, 0·795 eV and 0·717, 0·724 eV. This emission has not been observed in the floating zone purified silicon, which further substantiates the belief that it originates from an oxygen containing complex (Johnson and Compton 1971).

3.2. Temperature effects

The widths and peak energies of the prominent zero phonon lines are shown as a function of temperature in figures 2 and 3. The full lines through the experimental points have

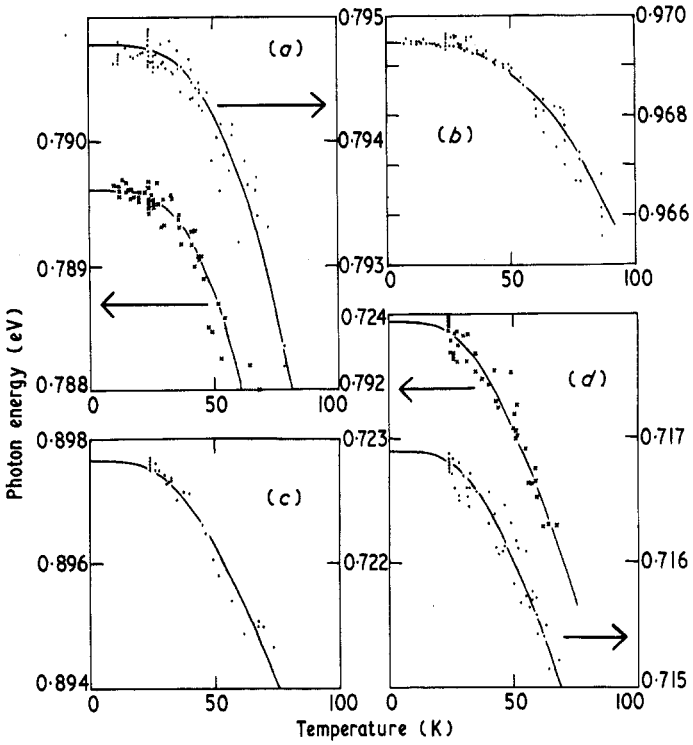

Figure 3. Measured and calculated energies of the zero phonon lines at (*a*) 0·790 and 0·795 eV, (*b*) 0·969 eV, (*c*) 0·898 eV, (*d*) 0·717 and 0·724 eV. In (*a*) and (*b*) the lines are calculated using the $\rho(w)$ shown in figure 6, and Debye spectra with cut off energies of 22 meV and 15 meV give closely similar lines. In (*c*) and (*d*) the calculation uses Debye spectra with cut off energies of 16 meV.

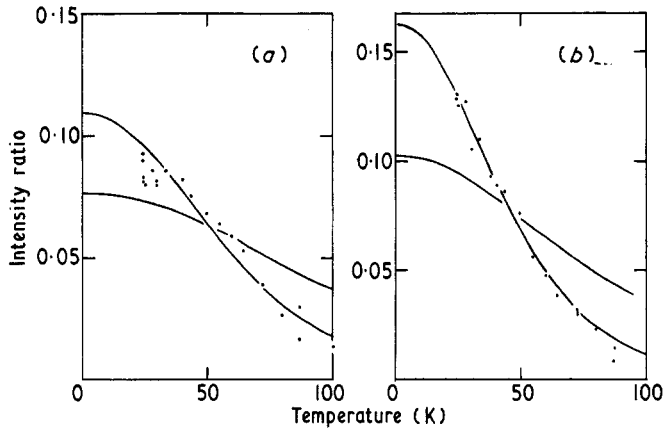

Figure 4. Measured and calculated ratios of the integrated transition probabilities of the zero phonon lines relative to their total associated band probabilities for (*a*) the 0·790, 0·795 eV band, (*b*) the 0·969 eV band. In (*a*) the sum of the 0·790 and 0·795 eV lines has been used. The accurately fitting lines are calculated with Debye spectra with cut off energies 22 and 15 meV respectively. The badly fitting lines are calculated from the $\rho(w)$ in figure 6.

been calculated as described in § 3.4. The total intensities of the emission bands decrease reversibly with increasing temperature above 25 K. By 100 K the integrated intensities of the bands associated with the 0·969 eV and 0·790, 0·795 eV lines are respectively 4% and 2% of their values at 25 K. In addition, the fraction of the emission in the zero phonon lines decreases as shown in figure 4. Previously, Jones and Compton (1971) have reported the temperature dependence of the width of the 0·790 and 0·969 eV lines. Our data are in agreement.

3.3. Discussion of the low temperature spectral shapes

The shapes of the spectra indicate that the electronic orbitals involved at the centres are localized within a very few atomic distances of the centres. This is seen on comparison with the bound exciton recombination luminescence from neutral donors and acceptors in silicon (Dean *et al* 1967). There the emission occurs in the photon range $\sim 1{\cdot}0$ to $\sim 1{\cdot}2$ eV, with the involvement of transverse optic phonons very similar to those that conserve momentum in intrinsic emission. These bound excitons may be pictured as a hole at the valence band maximum and an electron at the conduction band minima at $\boldsymbol{k} = (0{\cdot}82, 0, 0)$ (Dumke 1960). Although the 0·969, and 0·790 eV transitions do couple to transverse acoustic phonons of this wavevector (energy ~ 19 meV: Solbrig 1970), there is clearly no simple selection of phonons occurring (figure 1). It is appropriate, therefore, to discuss the shape of the spectra in terms of a point defect, quasimolecular, approach, rather than through perturbed band states.

The existence of vibronic, as opposed to electronic, spectra is due to electron–phonon coupling. The exact shape of the spectrum is determined by the nature of the coupling. Thus an electron–phonon interaction that is linear in the lattice displacement gives a different spectral shape from a strong quadratic interaction (eg Kiel 1965), while linear coupling itself may be of totally symmetric form (eg Maradudin 1966) or give Jahn–Teller distortions (eg Longuet-Higgins *et al* 1958).

Absorption lines at 0·790, 0·795 and 0·969 eV have not been observed in this work, or in any other, so that the nature of the coupling cannot be determined by comparing the absorption and emission spectra. Instead we note that the widths of the zero phonon lines (figure 2) increase by typically 2 meV between 0 and 75 K. This is the same magnitude (relative to the Raman energy) as observed over the same temperature range (relative to the Debye temperature) at vibronic centres in diamond (Davies 1970 and unpublished calculations), for which the quadratic coupling terms are small.

We cannot exclude the existence of a Jahn–Teller coupling, although the emission spectra do not show 'double peaked' phonon assisted bands. In the remainder of this paper we will investigate how closely the data may be described using the theories based on the adiabatic approximation (eg Maradudin 1966). One reason for doing this is that at both the centres providing the luminescence in figure 1 there are electronic levels whose energy separation is not large compared with the energies of the coupled phonons. Thus the 0·969 and 0·898 eV lines have a separation only 9% larger than the Raman energy of silicon (Dolling and Cowley 1966, Solbrig 1970), and so, if the initial state of the transitions is the same, the final states have this separation. The inset in figure 1 shows a very similar spacing between some of the levels. The coupling of the nearby electronic states by the electron–phonon interaction breaks down the validity of the adiabatic approximation, and although no detailed theory of the effect exists, we may expect that the standard adiabatic approximation would be on the point of breakdown when the electronic states have a separation of just larger than the phonon energies

involved. These emission bands may, therefore, provide an example of the behaviour of vibronic bands on the point of breakdown of the adiabatic approximation by this effect.

Using the adiabatic approximation it is possible to write analytical expressions for the shape of the spectrum (eg Pryce 1965, Maradudin 1966). The transition probability for the transition at a frequency ν is

$$W(\nu) = \sum_{n=0}^{\infty} W_n(\nu) \tag{1}$$

where the transition probability of an n-fold phonon process $W_n(\nu)$ has a relative integrated strength

$$\int d\nu \, W_n(\nu) = \exp(-S) \cdot \frac{S^n}{n!} \tag{2}$$

S, the Huang–Rhys factor, may be experimentally determined from the transition probability of the zero phonon line and that of the full band:

$$S = \ln\left(\frac{\sum_{n=0}^{\infty} \int d\nu \, W_n(\nu)}{\int d\nu \, W_0(\nu)}\right) \tag{3}$$

The transition probability of an n phonon process is the $(n-1)$th convolution of the

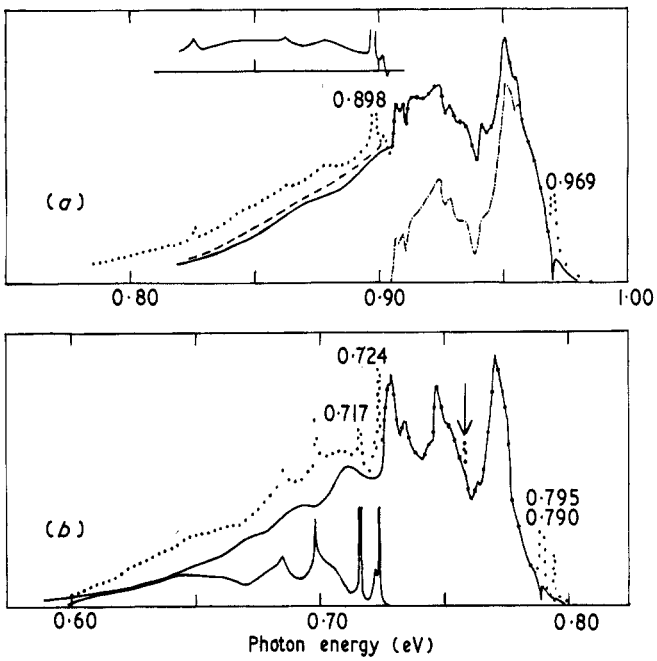

Figure 5. (*a*) Experimental spectrum measured at 26 K of the 0·969 eV and 0·898 eV bands (dotted curve). Subtraction of the assumed 0·898 eV band leaves the broken curve. The calculated fit is shown by the full curve and the emission involving one phonon by the chain curve. Inset is the difference of the measured (dotted curve) and calculated (full curve) spectra. (*b*) Spectrum of the 0·790, 0·795 eV and 0·717, 0·724 eV bands as measured at 24 K (dotted curve). The arrowed feature at 0·759 eV is an extra zero phonon line. The calculated spectrum is shown by the full curve. Inset is the difference of the measured and calculated spectra.

one phonon process $W_1(\nu)$. Thus $W_1(\nu)$ and S define the spectrum. If a $W_1(\nu)$ is guessed and S measured, a spectrum may be calculated and compared with experiment. Successive iterations enable a suitable $W_1(\nu)$ to be obtained that fits the spectrum. The results of the calculation are presented here in terms of a weighted frequency distribution $\rho(w)$ which is related to $W_1(\nu)$ by (Maradudin 1966):

$$W_1(\nu) = \text{constant} \times \exp(-S)\{n(\nu - \nu_0) + 1\}\frac{\rho(\nu - \nu_0)}{(\nu - \nu_0)^2} \tag{4}$$

where

$$n(x) = \left\{\exp\left(\frac{hx}{kT}\right) - 1\right\}^{-1}$$

and ν_0 is the zero phonon frequency.

Before comparing the calculated and experimental spectra it is necessary to allow for the effects of crystal perturbations, which broaden the observed spectrum. This, and (to a good approximation) the thermal broadening of the spectrum discussed below, may be allowed for by taking a convolution of the calculated spectrum with the observed zero phonon line.

Taking first the band associated with the 0·969 eV line, we note that because the 0·898 eV line has an integrated intensity 9 % of the 0·969 eV line it makes an appreciable contribution to the emission below 0·90 eV. If it is assumed that the 0·898 eV line has exactly the same phonon coupling as the 0·969 eV line, subtracting the assumed 0·898 eV contribution gives the approximate shape to the 0·969 eV band shown in figure 5*a*. The

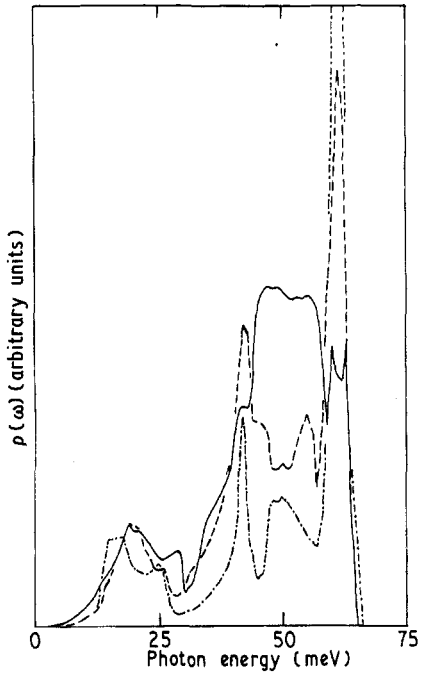

Figure 6. Densities of coupled phonon states for the 0·969 eV band (full curve) and the 0·790, 0·795 eV band (broken curve) compared with the phonon energy times the perfect lattice density of phonon states (chain curve).

Huang–Rhys factor for the 0·969 eV line is then found to be $S \sim 2{\cdot}06$ at 26 K. After performing the iterative computations described above, the experimental spectrum of figure 5*a* may be fitted quite well, as shown by the solid line, using the derived $\rho(w)$ shown in figure 6.

Unfortunately the 0·717 eV line has an obviously different phonon coupling from the 0·790 eV line (figure 1). The calculated fit to the band (figure 5*b*) is selfconsistent, in that the Huang–Rhys factor used ($S \sim 2{\cdot}35$) in calculating the spectral shape is also that which is obtained from equation 3 using the area enclosed under the calculated curve in the numerator of the right hand side of equation 3. However, the $\rho(w)$ used in the calculation (figure 6) cannot be claimed to be unique, although the energies of the peaks in the $\rho(w)$ must be correct. In performing the calculation, both lines in the 0·790, 0·795 eV doublet have been assumed to have the same phonon coupling so that the observed spectrum is the sum of two shifted bands of different strengths.

3.4. Analysis of the temperature dependence

Temperature changes in the emission spectra may arise through electronic or vibrational effects. One simple electronic effect is the change in charge state of a centre, due to its ionization, for example. Another example is the redistribution of electrons among the energy levels of the centre. Both examples may result in the appearance of new bands or the quenching of the luminescence. Electronic temperature effects are thus generally characterized by changes in the emission intensity. The rapid fall-off in emission from 25 to 100 K (§ 3.2) is, therefore, probably electronic in origin, but since both the 0·969 and 0·790, 0·795 eV bands fall off at comparative rates it is unlikely that the cause is either of the examples above, since this would require very similar electronic energy bands at these two dissimilar centres. It is possible that other defects in the crystals are involved, but detailed studies of the decrease in emission have not been made.

The temperature effects of electron–phonon coupling show up predominantly in the spectral distribution of the emission rather than its intensity—linear and quadratic electron–phonon coupling leave the integrated transition probability of a band unchanged (Maradudin 1966). The temperature dependence of the Huang–Rhys factor is

$$S = \text{constant} \times \int \frac{\mathrm{d}w\, \rho(w)\{2n(w) + 1\}}{w^2} \tag{5}$$

and is particularly noticeable by a weakening of the zero phonon line. Using standard assumptions concerning the magnitude of the quadratic electron–phonon coupling relative to the linear coupling, the width Γ of a zero phonon line may be written in terms of $\rho(w)$ as

$$\Gamma = a_1 \int \mathrm{d}w\{\rho(w)\}^2 n(w)\{n(w) + 1\} \tag{6}$$

The energy of the zero phonon line changes by

$$\Omega = a_2 \int \mathrm{d}w\, \rho(w)\{n(w) + \tfrac{1}{2}\} \tag{7}$$

and

$$\frac{a_1}{a_2^2} = \pi$$

In addition to these effects we must allow for the effects of crystal inhomogeneities and lattice thermal expansion. Usually the width of a zero phonon line is dominated, at low temperature (when $\Gamma \to 0$), by crystal inhomogeneities. At finite temperature, the observed lineshape is the convolution of the inhomogeneous broadening (which we assume is temperature independent) and the lorentzian phonon broadening (equation 6). The low temperature lineshapes in the present specimens are of 'bi-lorentzian' form:

$$I(v) = \{b + (v - v_0)^2\}^{-2}$$

The convolution of this with a lorentzian has been given analytically (Davies 1970). Using this tabulation, equation 6 may be fitted to the data. Thermal expansion gives an energy shift to the bands. The shift cannot be calculated since the hydrostatic strain coupling of the bands is unknown, but through the Gruneisen law it is closely proportional to Ω, equation 7 (Imbusch *et al* 1964). The temperature range of the present data only covers the range where the expansion coefficient is increasingly negative (Dolling and Cowley 1966). The measured shifts of all the zero phonon lines are proportional to the enthalpy of silicon, calculated from the data of Pearlman and Keesom (1952).

Fits of equations 5, 6, 7 to the data are given in figures 2, 3, 4 using the $\rho(w)$ of figure 6 and also using Debye spectra ($\rho(w) \propto w^3$, Maradudin 1966). The fits to the widths and energies of the 0·790, 0·795 and 0·969 eV lines using the $\rho(w)$ derived from the emission spectra are very good. However the fits to the intensities of the zero phonon lines are poor (figure 4). (In making the fit, equations 3 and 5 have been written as $I_0 = I_t k \exp(-S)$, where I_0 and I_t are the integrated transition probabilities of the zero phonon lines and the full band. The constant in equation 5 for S has been fixed using the measured values at low temperature. The constant k has been treated as a best fit parameter: ideally it would have the value $k = 1$.) The intensities of the zero phonon lines may be closely described by Debye spectra for $\rho(w)$, with maximum energies of ~ 20 meV. This energy is a very plausible value, considering the energy of the major peak in the $\rho(w)$ of figure 6. However, in this case the Debye approximation is misleadingly accurate, and evidently its use in parameterizing the temperature dependence of zero phonon lines can hide an inadequacy in the theory.

The success in fitting the widths and shifts, but not the intensities, of the zero phonon lines is probably due to the weighting of Γ and Ω (equations 6 and 7) to a small range of low values of w. In contrast, S (equation 5) depends on the entire spectrum and consequently may be far more affected by failure of the theory. It is interesting to note that a less detailed application of the same theory as used here to the F^+ centre in CaO (which shows a Jahn–Teller effect) also gives good fits to the width and energy, but not intensity, of the zero phonon line (Escribe and Hughes 1971).

Using the $\rho(w)$ obtained from the low temperature spectra, it should be possible to calculate the shape of the spectra at high temperature. This would be done (to a good approximation at not too high a temperature) by simply using equation 4 to obtain the part of the spectrum involving the emission of one phonon, $W_1(v)$, and calculating the corresponding part of the spectrum involving the absorption of a phonon from the lattice:

$$W_1^{\text{abs}}(v) = W_1(2v_0 - v) \exp\left\{\frac{-h(v - v_0)}{kT}\right\}$$

The total spectrum would then be generated using equations 1 and 2, with the appropriate high temperature value of S. However, we have seen that the temperature dependence of S cannot be calculated from $\rho(w)$ using the present theory, and so a fully selfconsistent

fit to the spectra cannot be obtained. On a practical level, the fact that the vibronic bands overlap creates further difficulties. However, if we again use the assumptions that the 0·898 eV line has exactly the same shape of phonon assisted band as the 0·969 eV line, and that these bands always have relative strengths of 1:11, then the calculated high temperature spectra of figure 7*b* are obtained when the *measured* values of S are employed. The smoothing out of the features in the band, and the weakening of the 0·95 eV peak, as the temperature increases is similar to that found experimentally (figure 7*a*). However a sharp peak at 0·933 eV (arrowed in figure 7*a*) is not reproduced in the calculation. This peak has not been studied—it is possibly another weak zero phonon line (the 80 K spectrum in figure 7*a* requiring $\sim$15 times higher gain than the 25 K spectrum).

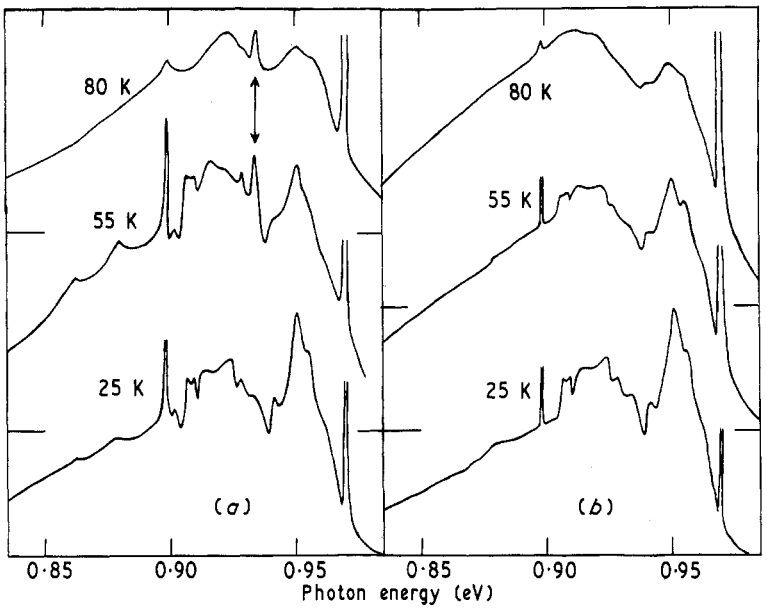

Figure 7. (*a*) The measured cathodoluminescence between 0·84 and 1·0 eV at 25, 55 and 80 K. (*b*) The spectra calculated at 25, 55 and 80 K using the measured values of S and assuming the 0·898 eV line has the same shape of phonon assisted band as the 0·969 eV line. The feature at 0·933 eV, arrowed in (*a*), is not reproduced in the calculation.

Finally, in figure 6 the calculated $\rho(w)$ are compared with the $\rho(w)$ that would result from unweighted coupling of the transitions to all the lattice phonons. It is interesting to note that a peak at 42 meV appears in the 0·790 eV coupling, and an inflexion occurs at that energy in the 0·969 eV coupling, corresponding to a sharp peak in the perfect crystal density of phonon states (Dolling and Cowley 1966). This peak does not derive from any major symmetry direction (Solbrig 1970).

4. Summary

Crucible grown and high purity floating zone purified silicon has been irradiated at room temperature using γ radiation. High resolution cathodoluminescence spectra of

the vibronic bands with zero phonon lines at 0·717, 0·724, 0·790, 0·795, 0·898 and 0·969 eV have been given. The widths and energies of these lines, and the intensities of the 0·790, 0·795 and 0·969 eV lines relative to the total intensities of their associated bands, have been given in the temperature range 25 to 75 K. An attempt to describe these data, using the simplest (adiabatic approximation) theory of the bands is partly successful, but the intensities of the zero phonon lines cannot be fitted using the spectra of coupled phonons derived from the emission spectra. It is not yet known whether this failure is due to a Jahn–Teller effect or to the coupling of electronic states whose separation is not much greater than the energies of some of the phonons interacting with the transitions.

Acknowledgments

We wish to thank the Royal Society and the University of London Central Research Fund for financial assistance, and C E Jones and E C Lightowlers for helpful discussions. One of us (APGH) is grateful to the SRC for a Research Studentship.

Note added in proof. Recent measurements have confirmed that the peak at 0·933 eV (figure 7*a*) does not occur at the same optical centre as the 0·969 eV line—the ratio of the strengths of the lines is specimen dependent.

References

Almeleh N and Goldstein B 1966 *Phys. Rev.* **149** 687–92
Davies G 1970 *PhD Thesis* University of London
Dean P J, Haynes J R and Flood W F 1967 *Phys. Rev.* **161** 711–29
Dolling G and Cowley R A 1966 *Proc. Phys. Soc.* **88** 463–94
Dumke W P 1960 *Phys. Rev.* **118** 938–9
Escribe C and Hughes A E 1971 *J. Phys.* C: *Solid St. Phys.* **4** 2537–49
Imbusch G F *et al* 1964 *Phys. Rev.* **133** A1029–34
Jones C E and Compton W D 1971 *Radiation Effects* **9** 83–8
Johnson E S and Compton W D 1971 *Radiation Effects*
Kiel T H 1965 *Phys. Rev.* **140** A601–17
Longuet-Higgins H C, Opik U, Pryce M H L and Sack R A 1958 *Proc. R. Soc.* A **244** 1–16
Maradudin A A 1966 *Solid St. Phys.* **18** 392–420 (New York: Academic Press)
Pearlman N and Keesom P H 1952 *Phys. Rev.* **88** 398–405
Pryce M H L 1965 *Phonons in Perfect Lattices and in Lattices with Point Imperfections* ed R W H Stephenson (London: Oliver and Boyd)
Roberts J K and Miller A R 1960 *Heat and Thermodynamics* (London: Blackie) p 521
Solbrig A W 1970 *J. Phys. Chem. Solids* **32** 1761–8
Spry R J and Compton W D 1968 *Phys. Rev.* **175** 1010–20
Watkins G D and Corbett J W 1965 *Phys. Rev.* **138** A543–55
Yukhnevitch A V 1965 *Sov. Phys.–Solid St.* **7** 259–60
Yukhnevitch A V and Tkachev V D 1966 *Sov. Phys.–Solid St.* **8** 1004–5
Yukhnevitch A V, Tkachev V D and Bortnik M V 1967 *Sov. Phys.–Solid St.* **8** 2571–4